This is the Pre-Published Version.
Z. Song, X. Huang, J. Jiang, X. Pan (2020) *A laboratory approach to CO2 and CO emission factors from underground coal fires*, International Journal of Coal Geology, 219, 103382. https://doi.org/10.1016/j.coal.2019.103382

A laboratory approach to CO_2 and CO emission factors from underground coal fires

Zeyang Song[a,b,*], Xinyan Huang[c], Juncheng Jiang[a,b,d], Xuhai Pan[a,b,*]

[a] *College of Safety Science and Engineering, Nanjing Tech University, 211816 Nanjing, PR China.*

[b] *Jiangsu Key Laboratory of Hazardous Chemicals Safety and Control, Nanjing Tech University, 211816 Nanjing, PR China.*

[c] *Department of Building Services Engineering, The Hong Kong Polytechnic University, ZS 832, BLK Z, Hong Kong, PR China.*

[d] *School of Environmental and Safety Engineering, Changzhou University, 213159 Changzhou, PR China.*

Abstract

Carbon emissions from underground coal fires (UCF) have become an emerging research topic and their role in global climate warming has been widely debated. Currently, one big uncertainty for assessing UCF's carbon emission is the hypothesized carbon emission factors (EF) from the complete combustion of coal, while the EF of smoldering combustion of coal in the context of UCF is still unknown yet. In this work, a 1/20 scale laboratory experimental framework was proposed to characterize transient carbon emissions and quantify EF_{CO2} and EF_{CO}. Effects of fire depth, ventilation area (aperture size), and coal rank on carbon emissions were explored with the extrapolation to the full-scale UCF. Results showed that total carbon emissions increase with the carbon content of coal. Volatile content is an important factor impacting the burning behavior and gas emission. Stable EF_{CO2} and EF_{CO} of UCF, independent of the fire depth and aperture size, were estimated as 2006±36 g kg^{-1} and 345±132 g kg^{-1}, respectively; its combustion efficiency was 85%±3%. The extrapolation of experimental data estimates the CO_2 emission of coal fires in China and the USA as 2.34×10^7 - 4.61×10^7 t yr^{-1}, which accounted for 0.4% - 0.9% of total CO_2 emissions in the world in 2016.

Keywords: greenhouse gas (CO_2); carbon monoxide (CO); incomplete combustion; smoldering fires

1. Introduction

Underground coal fires (UCF) are sites of slow combustion (smoldering) of subsurface coal. Comparing to the flaming combustion, smoldering is flameless, slow, and incomplete combustion in the porous fuels (Rein, 2011; Rein, 2013, 2016). UCF not only devour enormous valuable coal resources, but also emit considerable greenhouse gases (GHGs) into the atmosphere (Hower et al., 2009; Hower et al., 2013; Kuenzer et al., 2007; Song and Kuenzer, 2014) (see Fig. 1). The contribution of GHGs of UCF to global climate warming has become an emerging and debatable topic. Extensive investigations have been devoted to quantifying UCF's carbon emissions (CO_2, CO, hydrocarbons (C_xH_y)) at different spatial scales (Dindarloo et al., 2015; Engle et al., 2012; Engle et al., 2011; Hower et al., 2009; Hower et al., 2011; Hower et al., 2013; O'Keefe et al., 2011). Carbon emissions of UCF at local scale had been estimated by the direct measurements of exhaust gases in the field (Engle et al., 2012; Hower et al., 2011; Hower et al., 2013; Ide and Orr Jr., 2011). The advantage of direct measurement is the first-hand information, but its shortcoming is the low efficiency and limited spatial scale (local fire zone). In order to assess carbon emissions of UCF at the regional scale, an integration method of

* Corresponding authors.
Email addresses: zeyang.song@njtech.edu.cn (Z. Song); xy.huang@polyu.edu.hk (X. Huang); xuhaipan@njtech.edu.cn (X. Pan).

remote sensing detection with basic knowledge in terms of coal combustion (e.g., CO_2 emission factor, EF_{CO2}) was proposed (Engle et al., 2011; Tetzlaff, 2004). As for the national or even global scale, carbon emissions of UCF can be assessed theoretically by the product of the burnt mass of coal and EF_{CO2} of incomplete combustion of UCF (Ide and Orr Jr., 2011; O'Keefe et al., 2010; van Dijk et al., 2011). However, carbon emission factors for incomplete combustion of coal in the context of UCF have not been quantified yet, thus, EF_{CO2} employed in almost all existing assessments of carbon emissions of UCF was hypothesized from the complete combustion of coal (O'Keefe et al., 2010; van Dijk et al., 2011). Clearly, this hypothesis is questionable for the incomplete smoldering combustion of coal in the context of UCF, which could lead to an overestimated carbon emission of UCF.

Fig. 1. Gas emissions from underground smoldering coal fires in the Wuda Coalfield, Inner Mongolia, P.R. China (Courtesy of Dr. Bo Yang).

Carbon emissions from coal dust and peat smoldering fires, which have been well quantified recently (Hu et al., 2019; Hu et al., 2018; Wu et al., 2017), cannot provide valuable reference to UCF because the carbon content, chemical kinetics, and heat-and-mass transfer in smoldering peat fires are different from UCF (Huang and Rein, 2014; Song et al., 2017a). Therefore, the present work aims to fulfill the knowledge gap, that is, quantifying carbon emission factors of UCF for incomplete combustion and assessing the carbon emission of UCF at the national scale.

2. Methods

2.1 Coal sample

Lignite (CF), high-volatile bituminous coal (CC) and anthracite coal (XA) were collected from the Chi Feng Coal Mine in the Inner Mongolia Region, the Chang Cun Coal Mine in the Henan Province, and the Xin'An Coal Mine in the Henan Province of P.R. China, respectively. It was reported that UCF occurred in these coal mines. The sampling procedure referred to the Chinese standard GB/T19494.1-2004. All coal samples were ply samples collected from underground mining work face, and immediately stored in air-proof plastic buckets. In order to mimic *in-situ* UCF, fresh (no drying) and large coal particles were considered for laboratory experiments. Chunks of coal samples were crushed manually into particles. Then, they were filtered manually

using metal meshes. In this work, the diameter of coal particles was approximately 7 ± 2 mm.

The ultimate and proximate analyses of studied coal samples were presented in Table 1 (Song et al., 2017a; Song et al., 2017b). The proximate and ultimate analyses were conducted according to GB/T212-2008 (moisture, ash, and volatile contents), GB/T476-2008 (carbon (C) and hydrogen (H)), GB/T214-2007 (sulfur (S)), and GB/T19227-2008 (nitrogen (N)). The ultimate analyses were tested by the Elementar (vario EL cube, Germany). The fixed carbon content of the samples ranged between values for coals burned in the Wuda Coalfield (~60%) (van Dijk et al., 2011) and values obtained for the Truman Shepherd Coalfield (~70-80%) (O'Keefe et al., 2010).

Table 1 Molecular formula, ultimate and proximate analyses of the studied coal samples.

Basic properties		Lignite (CF)	Bituminous (CC)	Anthracite (XA)
Proximate analysis (dry basis, wt.%)	Moisture	26.07	2.86	1.74
	Volatile	29.98	34.75	12.33
	Ash	6.05	14.84	14.12
	Fixed carbon (by diff.)	37.90	47.55	71.81
Ultimate analysis (Dry ash-free basis, %)	Carbon	50.091	71.104	88.077
	Hydrogen	5.582	5.438	4.752
	Oxygen (by diff.)	42.370	21.880	3.990
	Nitrogen	0.894	1.313	1.680
	Sulfur	1.063	0.265	1.501
Molecular formula		$C_{1.58}H_{2.11}O$	$C_{4.33}H_{3.98}O$	$C_{29.43}H_{19.06}O$

2.2 Experimental setup

Propagation and extinction of subsurface smoldering fires are controlled by the heat and air (oxygen) transfer. For smoldering peat fire near ground (Huang et al., 2016) and the self-sustaining smoldering treatment of organic wastes (Zanoni et al., 2019a, b, c), heat transfer may play a dominant role. However, UCF is mainly controlled by the air transport due to deplete oxygen atmosphere at underground while thermal insulation is formed by underground rocks/sediments. The natural driving forces of fresh air transport to UCF include wind, atmospheric pressure fluctuation (Song et al., 2015), and topographic effect (Song et al., 2014). However, with only these natural air flow, the oxygen supply to underground space should decay with increasing the fire depth, and UCF is expected to be smothered at certain fire depth before burnout. However, the long-last UCF suggests the existence of some other air-supply mechanism. Recent field work (Krevor et al., 2011) and laboratory experiments (Li et al., 2018;) demonstrated that the buoyancy-driven natural convection (i.e., the chimney effect) is a significant air-supply mechanism in UCF.

In this work, buoyancy-driven natural ventilation for UCF was considered, while the atmospheric pressure fluctuation and topographic effect were excluded. An experimental research framework, as shown in Fig.2 (Song et al., 2019b), was proposed to simulate UCF and parameterize the couplings of heat and gas transports as well as smoldering combustion. Air and smoke transport channels were constructed using a ‘U-shaped’ steel-stainless pipes (diameter, 6 cm). A combustion reactor (diameter, 12 cm) was connected between air and

smoke transport channels. The top horizontal surface was viewed as the ground surface (H=0 m), then the space below was considered to be underground.

For a given coal rank, carbon emissions from UCF are controlled by air supply, which is impacted by fire depth (H) and ventilation channel size (aperture diameter (Φ) in this work). In the field, the fire depth is less than 90 m (Shi et al., 2017) and the channel width ranges from several centimeters to hundreds of centimeters (Kuenzer and Stracher, 2012). The experimental framework allowed to vary fire depth (H=-1.6 m - 3.6 m) via adjusting the vertical lengths of transport pipes and aperture size (Φ=1 and 4 cm) via a hollow plug. Previous scale analysis demonstrated that the laboratory scale was representative for a 1/20 scale of UCF in the field (Song et al., 2019b).

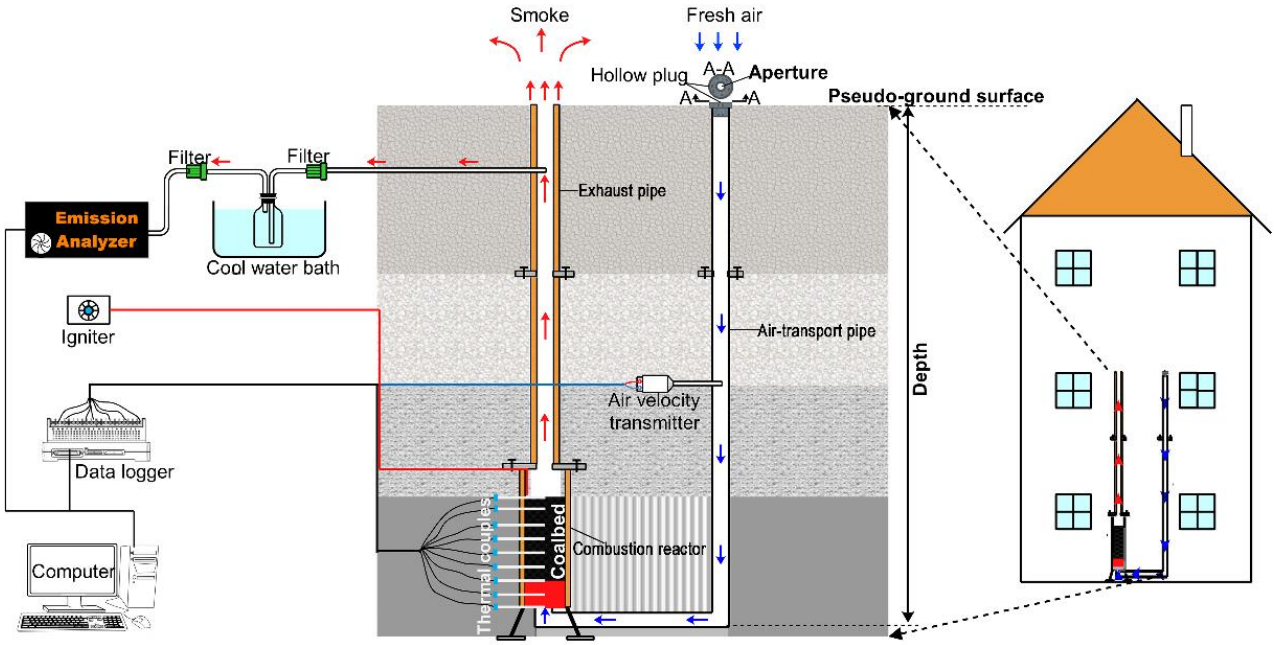

Fig. 2. Schematic diagram of the experimental setup for the underground coal fire (UCF).

At a height of approximate 0.14 m, coal sample was homogeneously piled up in the reactor. An igniter (inconel cable, 220 V, 500 W) was placed under the coal bed to initialize forward smoldering. A small portion of smoke (1 ml min^{-1}) was pumped through a sampling tube to the Emission Analyzer (TESTO 350, Germany). The range and accuracy of the emission analyzer are: 0-25% and ±0.2% for O_2; 0-50% and ±0.3% for CO_2; 0-40% and ±4% for CO, respectively. Sensors of O_2 (CO) and CO_2 are electrochemical and infrared, respectively. Before entering the gas analyzer, the exhaust-gas sample was cooled through a water bath, and the contaminative products such as tar-containing vapor and particle materials were removed by filters. Seven thermocouples (K type, OMEGA, USA) (TC_1-TC_7) with a vertical interval of 2 cm were inserted along the center axis of the reactor to monitor burning temperature and smoke temperature (TC_7). TC_1 was the closest thermocouple to the igniter. An anemometer (FMA900R, OMEGA, USA; range: 0-1.02 m/s, accuracy: ±2% FS) was employed to measure air velocity. All data were recorded at a rate of every 2 seconds (0.5 Hertz) and saved in a computer. Raw coal and ash mass were measured by an electrical balance. Each experiment was repeated at least 2 times. All experiments were conducted inside a large-scale laboratory to eliminate the influence of wind effect. Experimental procedures were elucidated in our previous work (Song et al., 2019b).

2.3 Estimating transient carbon emission factors

2.3.1 Chemical equation of smoldering combustion

Mass of raw coal and residuals after burning were weighed by a precision balance. Comparing the ratio of residuals mass to raw coal mass with the ash content from the proximate analysis, mass fraction of char in residuals can be identified. Chemical equations of smoldering combustion with or without char residuals are determined in the following.

(a) Residuals without char (bituminous coal (CC) and lignite (CF)): Experiments of bituminous coal (CC) and lignite (CF) showed that ash mass accounted for ~13% and ~6% of total raw coal mass respectively, which consists with that based on the proximate analysis (Song et al., 2017a; Song et al., 2017b). This result indicates that raw coal was completely converted into gaseous products including CO_2, CO, and C_xH_y. Experimental results of exhaust gases show that concentrations of CO_2 and CO were far greater than C_xH_y. Hence, we assume that raw coal was merely converted to CO_2 and CO. Smoldering combustion of UCF is simplified into a global one-step heterogeneous oxidation:

$$C_xH_yO_z + \left(\frac{y}{4} + a + \frac{b}{2} - \frac{z}{2}\right) O_2 \rightarrow aCO_2 + bCO + \frac{y}{2}H_2O \quad (1)$$

According to the mass conservation:

$$a + b = x \quad (2)$$

Besides,

$$\frac{a}{b} = \frac{X_{ex,CO2}}{X_{ex,CO}} = \eta \quad (3)$$

where $X_{ex,CO2}$ and $X_{ex,CO}$ denote CO_2 and CO volume concentrations (vol.%) in exhaust gases.

Then, *a* and *b* can be written as

$$a = \frac{x}{1+1/\eta} \quad (4)$$

$$b = \frac{x}{1+\eta} \quad (5)$$

(b) Residuals with char (anthracite coal (XA)): Experiments of anthracite coal (XA) showed that the mass fraction of residuals was much higher than that of ash from the proximate analysis, indicating that a portion of char was unburnt and remained in residuals. Carbon should be involved in the chemical equation, if char is present in residuals. Thus, the chemical equation can be written as:

$$cC_xH_yO_z + dO_2 \rightarrow aCO_2 + bCO + eH_2O + fC \quad (6)$$

According to the mass conservation, the stoichiometric coefficients can be obtained in the following.

$$c = \frac{m_{coal}}{12x+y+16z} \quad (7)$$

$$f = \frac{m_{residuals} - m_{coal}Y_{ash}}{12} \quad (8)$$

$$a = \frac{cx-f}{1+1/\eta} \quad (9)$$

$$b = \frac{(cx-f)}{1+\eta} \quad (10)$$

$$e = \frac{cy}{2} \quad (11)$$

$$d = \frac{(2+\eta)a+e-cz}{2} \quad (12)$$

2.3.2 Transient carbon emission factors

With chemical equations above, the transient carbon emission factors are derived:

(a) Residuals without char (bituminous coal (CC) and lignite (CF))

According to Eq. (1):

$$\Delta\dot{m}_{CO2} = \frac{44a}{12x+y+16z}\dot{m}_F \tag{13}$$

$$\Delta\dot{m}_{CO} = \frac{28b}{12x+y+16z}\dot{m}_F \tag{14}$$

where $\dot{m}_F$ is the burning rate of coal in kg s^{-1}. $\Delta\dot{m}_{CO2}$ and $\Delta\dot{m}_{CO}$ denote released CO_2 and CO mass flow rates in kg s^{-1}, respectively.

Based on Eq. (13) and Eq. (14), CO_2 and CO emission factors can be expressed as:

$$EF_{CO2} = \frac{\Delta\dot{m}_{CO2}}{\dot{m}_F} = \frac{44a}{12x+y+16z} \tag{15}$$

$$EF_{CO} = \frac{\Delta\dot{m}_{CO}}{\dot{m}_F} = \frac{28b}{12x+y+16z} \tag{16}$$

(b) Residuals with char (anthracite coal (XA))

Based on Eqs. (6), (13) and (14), CO_2 and CO emission factors can be expressed as:

$$EF_{CO2} = \frac{\Delta\dot{m}_{CO2}}{\dot{m}_F} = \frac{44a}{c(12x+y+16z)-12f} \tag{17}$$

$$EF_{CO} = \frac{\Delta\dot{m}_{CO}}{\dot{m}_F} = \frac{28b}{c(12x+y+16z)-12f} \tag{18}$$

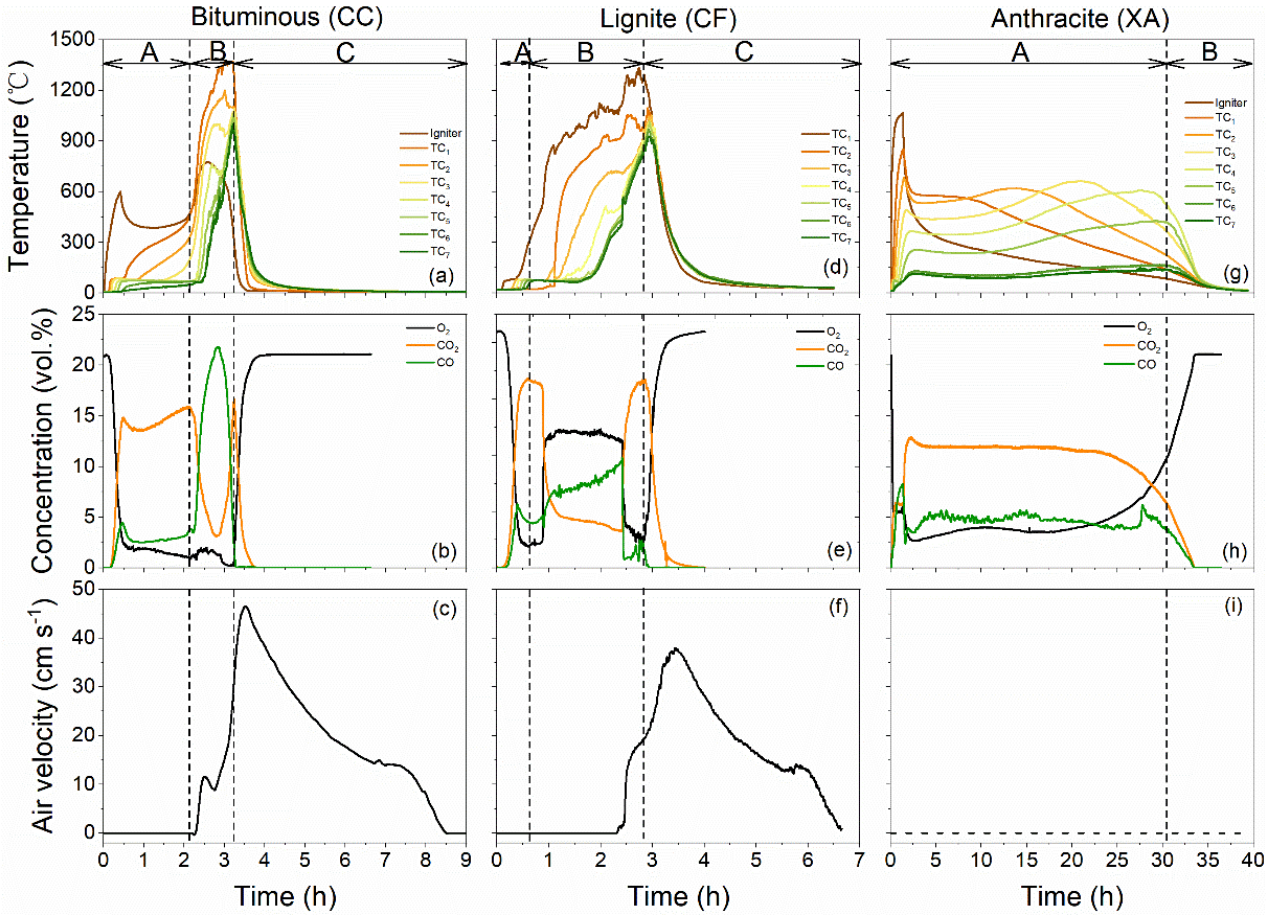

Fig. 3: Experimental histories of exhaust gases concentration (upper row), temperature (middle row), and air velocity (bottom row). (a) – (c): bituminous coal; (d) – (f): lignite; (g) – (i): anthracite coal.

3. Results and discussion

Figure 3 shows that bituminous coal and lignite share the similar behaviors of burning and gas emissions. Three stages (A, B, and C) associated with smoldering combustion of UCF are characterized. Taking bituminous coal with Φ= 4 cm at H=-2.6 m for instance, their characteristics are detailed in the following. However, UCF of anthracite coal behaves differently from the bituminous coal and lignite. The effect of coal rank is discussed in Section 3.4.

3.1 Smoldering combustion of UCF

At the first stage (A), after the igniter (T_{ig}=600 °C) was turned off, $X_{ex,CO2} \approx 15\%$ and $X_{ex,CO} \approx 3\%$; the temperature of the coal layer close to the igniter continually increases. This result indicates that self-sustaining smoldering combustion is established, although air velocity is too small to be measured due to weak thermal buoyancy at low temperature and negative solutal buoyancy resulting from heavy exhaust gases ($\Delta M = M_{air} - M_{smoke} < 0$ g mol^{-1}) (Song et al., 2019b).

At the second stage (B), smoldering combustion is facilitated by faster air velocity, which releases more thermal energy and further enhances natural convection. These two positive feedbacks between combustion and natural ventilation maintain until coal burns out. The thermal convection becomes stronger with higher air velocity, which promotes the pyrolysis of the upper coal layer. Hence, $X_{ex,CO}$ increases highly to ~22% and $X_{ex,CO2}$ reduces to ~3%. After the pyrolysis is completed, char starts to burn. Then $X_{ex,CO2}$ increases back to ~15% and $X_{ex,CO}$ drops to zero. The peaks of $X_{ex,CO2}$ and burning temperature indicate the end of smoldering combustion. It's worth mentioning that peak temperature of smoldering combustion in the context of UCF is over 1300 °C, which is higher than most of organic materials such as coal tar (Switzer et al., 2009; Switzer et al., 2014), peat (Huang and Rein, 2014, 2017; Yang et al., 2016; Yang et al., 2019), and polyurethane foam (Torero and Fernandez-Pello, 1996). The third stage (C) is the burnout of coal. Temperature decreases to the ambient temperature, and smoke ($X_{ex,CO2}$) is diluted and finally replaced by fresh air.

3.2 Transient CO_2 and CO emission factors

Transient EF_{CO2} and EF_{CO} are estimated by Eqs. (15) and (16), and depicted in Fig. 4. Light areas and bold lines denote the range and the average of emission factors estimated from replicated experiments, suggesting a good repeatability.

The evolution of the *EF* with the burning temperature (TC_2) shown in Fig. 4 can also be divided into three stages in the following. Note that TC_2's temperature is used to represent the burning temperature, instead of TC_1 to avoid the influence of the igniter.

The first stage (I): stable $X_{ex,CO}/X_{ex,CO2}$. EF_{CO2} and EF_{CO} are almost stable at 2200 and 250 g kg^{-1}, respectively. At this stage, EF_{CO2} is almost an order magnitude greater than EF_{CO}. The duration of this stage is in accordance with the first stage of smoldering combustion, as mentioned before.

The second stage (II): increasing $X_{ex,CO}/X_{ex,CO2}$. With increasing burning temperature, EF_{CO} (EF_{CO2}) is linearly increased (decreased) by ~1000 g kg^{-1} (~1500 g kg^{-1}). At the burning temperature of ~800 °C, EF_{CO} exceeds EF_{CO2}. At this stage, pyrolysis plays a dominant role in carbon emissions. The duration of this stage is in line with the earlier period of the second stage of smoldering combustion.

The third stage (III): decreasing $X_{ex,CO}/X_{ex,CO2}$. With increasing burning temperature, EF_{CO} sharply drops to ~750 g kg^{-1}; EF_{CO2} rapidly rises back to ~1500 g kg^{-1} ($X_{ex,CO2} \approx 15\%$, see Fig. 3a). At this stage, pyrolysis is basically completed and char combustion is the predominant reaction. Thus, EF_{CO2} is larger than EF_{CO}. The duration of this stage overlaps the later period of the second stage of smoldering combustion.

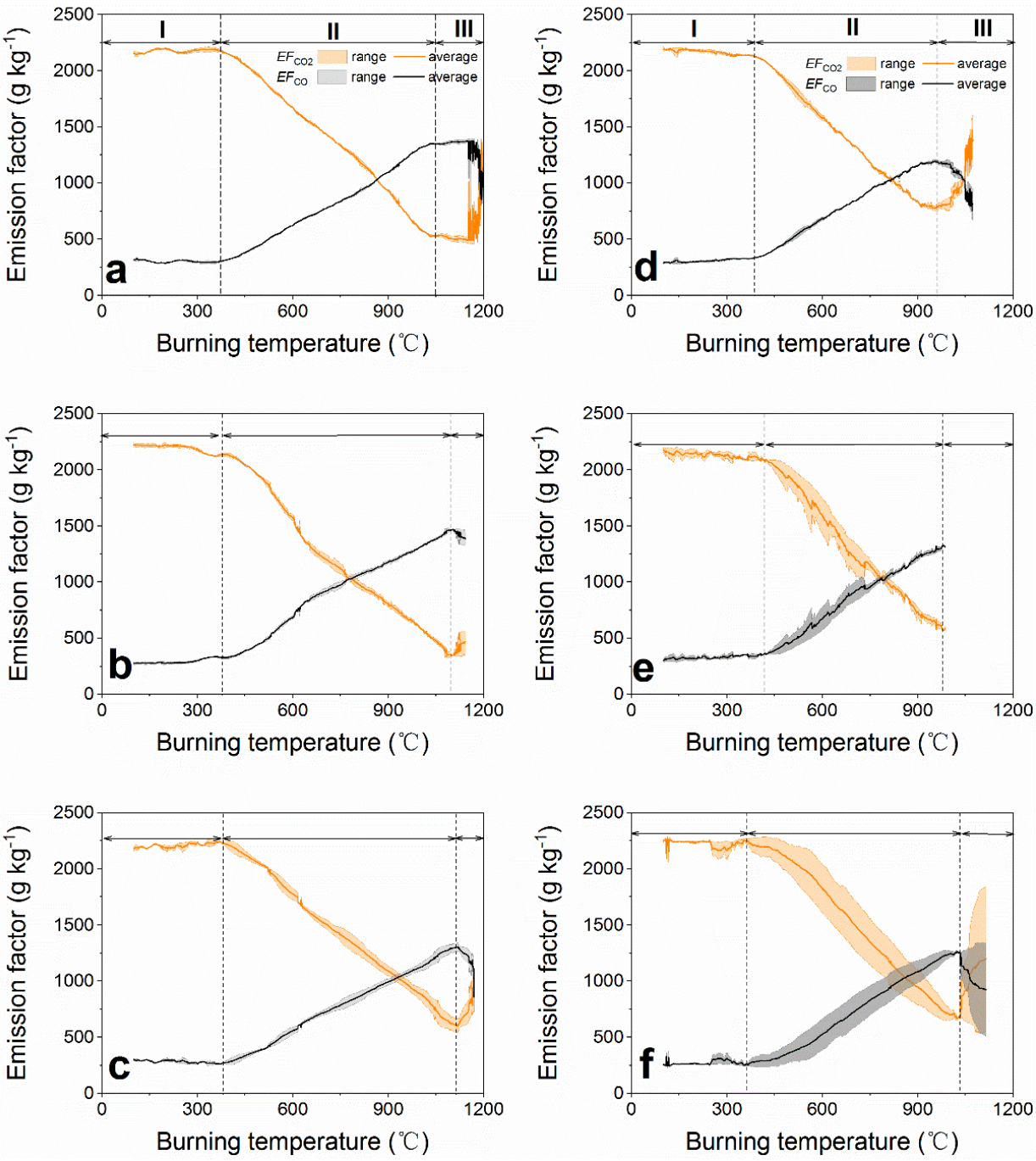

Fig. 4. Transient CO_2 and CO emission factors of UCF: (a) H=-1.6 m and Φ= 4 cm; (b) H=-2.6 m and Φ= 4 cm; (c) H=-3.6 m and Φ= 4 cm; (d) H=-1.6 m and Φ= 1 cm; (e) H=-2.6 m and Φ= 1 cm; (f) H=-3.6 m and Φ= 1 cm. Bold line: average value of two replicated experiments; Range: maximum-minimum values of two replicated experiments.

The maximum burning temperature indicates the end of smoldering combustion. Afterwards, temperature drops to the ambient temperature and smoke ($X_{ex,CO2}$ and $X_{ex,CO}$) is diluted and finally replaced by air. The emission at this burnout stage is not presented in Fig. 4.

Transient emission factors analyzed in this work indicate that the carbon emission of UCF fed by natural ventilation is very dynamic and depends on both burning temperature and air availability. Of course, carbon content (coal rank) also exerts an important influence on carbon emission (see Section 3.4). In addition, fire depth and aperture size impact air transport, which is expected to impact carbon emissions of UCF.

3.3 Effects of fire depth and aperture size

Figure 5 shows the effects of fire depth and aperture size on average emission factors ($\overline{EF}_{CO2}$ and $\overline{EF}_{CO}$). At the stage I, regardless of fire depth or aperture size, air velocity is slow so that it cannot be determined from the anemometer, as shown in Fig 3c. This result suggests that fire depth and aperture size have minimal influence on natural ventilation at the stage I. Smoldering combustion of UCF is mainly controlled by air transport. Under a similar air velocity, the kinetics and emissions of smoldering combustion of UCF at the stage I are independent on fire depth and aperture size. Thus, as shown in Fig. 5a, both $\overline{EF}_{CO2}$ and $\overline{EF}_{CO}$ are stable at 2201.5 ± 15.2 g kg^{-1} and 284.3 ± 9.6 g kg^{-1}, respectively.

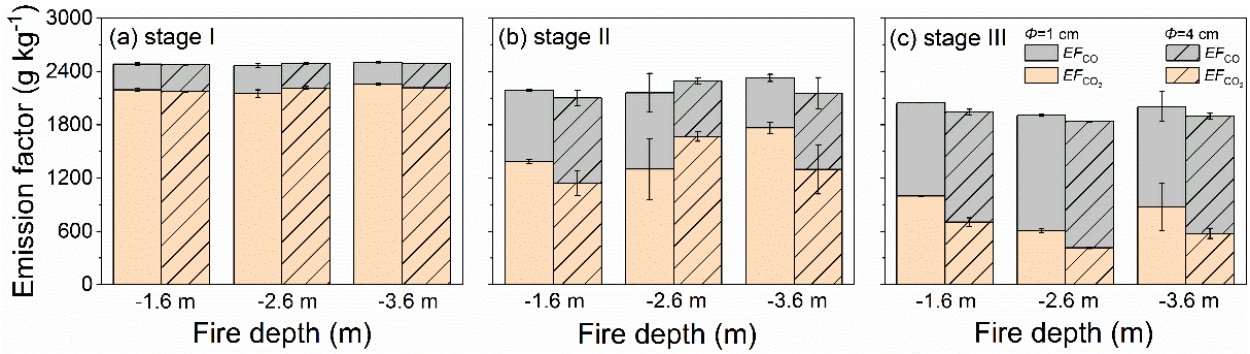

Fig. 5. Effects of fire depth and aperture size on carbon emissions at the stage (a) I, (b) II, and (c) III. Error bars denote the standard deviation of two replicated experiments.

At the stages II and III, natural ventilation is remarkably enhanced with increasing burning temperature (see Fig. 3c). The experimental results show that with an increase of aperture size, air velocity increases; with increasing fire depth, air velocity is basically invariable at the stage II, but increases significantly at the stage III (not shown in this work). As we analyzed before, hot smoke with low oxygen at a faster speed facilitates pyrolysis of coal layer above, resulting in higher $X_{ex,CO}$ and lower $X_{ex,CO2}$. Therefore, $\overline{EF}_{CO2}$ decreases with an increase of aperture size at both stages II and III, except for the stage II (H=-2.6 m).

Gases (CO_2, CO, O_2, CH_4, H_2, and N_2) from *in-situ* UCF in the Wuda Coalfield were measured (Schloemer, 2006). Cluster analysis showed that CO/CO_2 and O_2/CO_2 were independent of the gas temperature. The author interpreted that the sampled gases were partly diluted by air. Thus, CO_2 and CO concentrations obtained from *in-situ* UCF in the Wuda Coalfield may not be essentially comparable to those from the laboratory, although CO_2 concentrations in the field (up to 16.3%) (Schloemer, 2006) and the laboratory (up to 17% for the bituminous coal in this work) were close to each other. It also indicates that it's of significant for the laboratory approach to quantify the genuine CO_2 and CO concentrations from the incomplete combustion in the context of UCF, avoiding the influence of air dilution on exhaust gases emitted from UCF in the field.

3.4 Effect of coal rank

In this work, lignite (CF), bituminous coal (CC), and anthracite coal (XA) are considered. As can be seen from Fig. 3, anthracite coal shows a different mode of burning and gas emission, comparing to the lignite and bituminous coal. Fig. 3g suggests that the peak burning temperature (~650 °C) of anthracite coal is significantly lower than those for lignite and bituminous coal (~1300 – 1400 °C). This is attributed to very slow air velocity (<2 cm s^{-1}) so that it is unable to be measured by the anemometer (see Fig. 3i). Multiple peaks in Fig. 3g indicates that the smoldering fire front spreads along the coal bed. This phenomenon is associated with a high

mass fraction of residuals. It's worth to mention that the burning time of XA coal takes place over 30 h, almost nine times longer than CF and CC coal. Exhaust gas concentrations in the whole burning process for anthracite coal are stable ($X_{ex,O2}$≈3%, $X_{ex,CO2}$≈12%, and $X_{ex,CO}$≈5%). As shown in Fig. 3 g – i, two stages are defined for UCF of anthracite coal. The first stage (I) is the main period for stable burning; the second stage (II) is the burnout.

The volatile content of coal is the key factor determining different modes of burning behaviors and gas emissions, because permeability and gas flow resistance is greatly improved for lignite and bituminous coal (volatile content=30% - 34% in this work, see Table 1) when coalbed is shrunk due to gas release from the coal matrix. Improved permeability and decreased flow resistance lead to enhancing air supply, which facilitates the burning of coal and further increases air velocity. However, for the anthracite coal, volatile content is low (12.33%). Therefore, the coalbed is barely shrunk and gas flow resistance is still high, resulting in slow air velocity. In this circumstance, the burning temperature is low so that the char burns incompletely and remains in residuals.

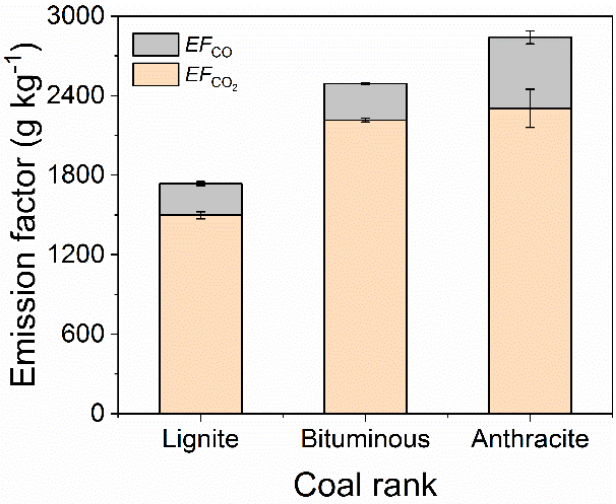

Fig. 6 Evolution of emission factors at the stage I with coal rank (Φ= 4 cm and H=-2.6 m). Error bars denote the standard deviation of two replicated experiments.

The stage I has a stable carbon emission process. The air velocity is low due to the thick coal bed, which could be applicable to the scenarios of the percolation channels in the field. Thus, carbon emission factors of three coal samples at this stage (Φ= 4 cm and H=-2.6 m) are compared to study the effect of coal rank. Figure 6 presents the dependence of carbon emission factors on coal rank. It indicates that, expectedly, the total carbon emission generally increases with the carbon content of coal. It seems that EF_{CO2} is remarkably larger but EF_{CO} almost keeps constant at 257±18 g kg^{-1}, comparing bituminous coal and lignite; on the other hand, EF_{CO} is significantly higher but EF_{CO2} barely changes (2260±44 g kg^{-1}), comparing anthracite coal and bituminous coal. The mechanism of this phenomenon requires a further study in the future.

3.5 Extrapolating to the full-scale UCF

Investigation on carbon emissions from pulverized coal combustion (Wu et al., 2017) may not be referred by the UCF with incomplete combustion. Effects of particle size, mass transport (air supply), and heat transfer on the carbon emission of UCF deserve a systematic investigation. These effects cause a large uncertainty when extrapolating from the laboratory-scale experiments to full-scale UCF. Key factor(s) must be captured while extrapolating or scaling analysis. In this work, we postulate that air supply is the single most important

factor, because it controls burning temperature, products (like carbon emissions (Yuan and Smith, 2011)), burning rate, and fire spread of UCF.

Our previous work (Song et al., 2019b) reported an empirical formula correlating the air velocity (V_a) with regard to the fire depth (h):

$$V_a = f_1(T_g)(2g|h|(1-\frac{T_a}{T_g}))^{f_2(T_g)} + f_3(T_g)(\frac{2g|h||M_a-M_g|}{M_a}) \quad (19)$$

where T_g, T_a, g, M_a, and M_g are smoke temperature, ambient temperature, gravitational acceleration, molar mass of air, and molar mass of smoke, respectively. In Eq. (19), the first term and the second term on the right-hand side denote the air velocity induced by thermal and solutal buoyancy forces, respectively.

Previous scaling analysis (Song et al., 2019b) also demonstrated that the formula is insensitive to the geometric scale but depends on the permeability of ventilation channels, as shown as follows:

$$\frac{V_{a,F}}{V_{a,M}} = \frac{K_F}{K_M} \quad (20)$$

where K is permeability, and subscripts F and M denote full scale and laboratory scale, respectively.

The permeability of coalbed in the laboratory is of the order magnitude of 10^{-7} m^2. Thus, the air velocity induced by UCF in the field could be extrapolated by the permeability of burning coal bed and Eqs. (19) – (20). Thus, the permeability of the ventilation channels must be considered if *EF* obtained from the laboratory-scale experiments are extrapolated for UCF in the field.

3.6 Comparing to peat smoldering fires

Stable carbon emissions at the stage I are chosen for comparing analyses and nation-scale estimation of CO_2 emission shown in next the section, because burning status and natural ventilation at the stage I are mostly close to the *in-situ* underground smoldering coal fires. A review by Hu et al. (Hu et al., 2018) reported that carbon emissions from tropical peat fires are higher than from boreal and temperate peat fires. $\overline{EF}_{CO2}$ and $\overline{EF}_{CO}$ of tropical peat (volatile content=56.0%) fires are approximately 1615 g kg^{-1} and 248 g kg^{-1}, respectively. They are quite close to the lignite (volatile content=30%) tested in this work ($\overline{EF}_{CO2}$=1498±26 g kg^{-1} and $\overline{EF}_{CO}$=239±15 g kg^{-1}). By contrast, $\overline{EF}_{CO2}$ and $\overline{EF}_{CO}$ of bituminous coal and anthracite coal are higher than those of tropical peat fires. From this point of view, the contribution of GHGs emitted from UCF to global warming cannot be neglected.

3.7 Reassessment of CO2 emissions from coal fires

van Dijk et al. (van Dijk et al., 2011) and O'Keefe et al. (O'Keefe et al., 2010) have assessed CO_2 emissions at the national scales of China and the USA. In their work, maximum combustion efficiency (~100% carbon converted to CO_2) were assumed and $\overline{EF}_{CO2}$=2560 - 3500 g kg^{-1}. This assumption is applicable for coal-power plants, but not for smoldering combustion of UCF and coal stockpiles. This experimental work demonstrates that $\overline{EF}_{CO2}$ was overestimated and the combustion efficiency should be reduced to 85.4%±3% ($\overline{EF}_{CO2}/(\overline{EF}_{CO2}+\overline{EF}_{CO})$) based on experimental data with three coal ranks in this research work. Assuming that the permeability of ventilation channels in the field is at the same magnitude order of 10^{-7} m^2 as in the laboratory, CO_2 emission from China and the USA is therefore updated to 1.07×10^7 - 2.14×10^7 t yr^{-1} and 1.17×10^7 - 2.47×10^7 t yr^{-1}, respectively. The CO_2 emission of coal fires in both China and the USA accounts for 0.4% - 0.9% of the total CO_2 emissions in the world in 2016 (527.4×10^7 t, assessed from *United States Environmental Protection Agency*).

4. Conclusions

An experimental research framework is proposed in this research to characterize transient carbon emissions and quantify CO_2 and CO emission factors of UCF for incomplete combustion. Lignite, bituminous coal, and anthracite coal are considered. Results show that transient carbon emissions in the whole duration of smoldering combustion are mainly determined by air velocity of natural ventilation induced by UCF. Despite of a slow airflow velocity, carbon emission is stable ($\overline{EF}_{CO2}$=2006±36 g kg^{-1} and $\overline{EF}_{CO}$=350±132 g kg^{-1}) and independent on fire depth and aperture size; with a high rate of gas flow, pyrolysis could be facilitated by upward thermal convection of gas flow, leading to higher CO emission. Anthracite coal burns much slower than lignite and bituminous coal, and its gas emission is generally stable during the whole burning process. The volatile content is a key factor determining the burning behaviors and gas emissions. Due to the high carbon content, the $\overline{EF}_{CO2}$ and $\overline{EF}_{CO}$ of bituminous coal and anthracite coal are higher than those of lignite and tropical peat fires. The previous estimate of CO_2 emission of coal fires is modified according to experimental data in this work. The CO_2 emission of coal fires in China and the USA accounts for 0.4% - 0.9% of the global CO_2 emissions in 2016.

Acknowledgments

This work was funded by the National Natural Science Foundation of China (No. 51804168 and No. 51876183), China Postdoctoral Science Foundation (No. 2018T110492 and No. 2017M620209), and Natural Science Foundation of Jiangsu Province (No.: BK20171005 and No. 17KJB620003). Thanks to Mr. Wenyu Qi for collecting coal samples. Experimental assistances of Mr. Xueliang Zhu, Mr. Dongxue Zhang Mr. Tiancheng He, and Mr. Maorui Li are appreciated. We gratefully acknowledge valuable comments from two anonymous reviewers and Dr. Jolanta Kus.

References

Dindarloo, S.R., Hood, M.M., Baghereih, A., Hower, J.C., 2015. A statistical assessment of carbon monoxide emissions from the Truman Shepherd coal fire, Floyd County, Kentucky. Int. J. Coal Geol. 144–145, 88-97.

Engle, M.A., Olea, R.A., O'Keefe, J.M.K., Hower, J.C., Geboy, N.J., 2012. Direct estimation of diffuse gaseous emissions from coal fires: Current methods and future directions. Int. J. Coal Geol. 112, 162-172.

Engle, M.A., Radke, L.F., Heffern, E.L., O'Keefe, J.M.K., Smeltzer, C.D., Hower, J.C., Hower, J.M., Prakash, A., Kolker, A., Eatwell, R.J., ter Schure, A., Queen, G., Aggen, K.L., Stracher, G.B., Henke, K.R., Olea, R.A., Román-Colón, Y., 2011. Quantifying greenhouse gas emissions from coal fires using airborne and ground-based methods. Int. J. Coal Geol. 88, 147-151.

Hower, J.C., Henke, K., O'Keefe, J.M.K., Engle, M.A., Blake, D.R., Stracher, G.B., 2009. The Tiptop coal-mine fire, Kentucky: Preliminary investigation of the measurement of mercury and other hazardous gases from coal-fire gas vents. Int. J. Coal Geol. 80, 63-67.

Hower, J.C., O'Keefe, J.M.K., Henke, K., Baghereih, A., 2011. Time series analysis of CO concentrations from an Eastern Kentucky coal fire. Int. J. Coal Geol. 88, 227-331.

Hower, J.C., O'Keefe, J.M.K., Henke, K.R., Wagner, N.J., Copley, G., Blake, D.R., Garrison, T., Oliveira, M.L.S., Kautzmann, R.M., Silva, L.F.O., 2013. Gaseous emissions and sublimates from the Truman Shepherd coal fire, Floyd County, Kentucky: A re-investigation following attempted mitigation of the fire. Int. J. Coal Geol. 116–117, 63-74.

Hu, Y., Christensen, E., Restuccia, F., Rein, G., 2019. Transient gas and particle emissions from smouldering

combustion of peat. Proc. Combust. Inst. 37, 4035-4042.

Hu, Y., Fernandez-Anez, N., Smith, T.E.L., Rein, G., 2018. Review of emissions from smouldering peat fires and their contribution to regional haze episodes. Int. J. Wildland Fire 27, 293–312.

Huang, X., Rein, G., 2014. Smouldering combustion of peat in wildfires: Inverse modelling of the drying and the thermal and oxidative decomposition kinetics. Combust. Flame 161, 1633–1644.

Huang, X., Rein, G., 2017. Downward spread of smouldering peat fire: the role of moisture, density and oxygen supply. Int. J. Wildland Fire 26, 907-918.

Huang, X., Restuccia, F., Gramola, M., Rein, G., 2016. Experimental study of the formation and collapse of an overhang in the lateral spread of smouldering peat fires. Combust. Flame 168, 393–402.

Ide, S.T., Orr Jr., F.M., 2011. Comparison of methods to estimate the rate of CO2 emissions and coal consumption from a coal fire near Durango, CO. Int. J. Coal Geol. 86, 95-107.

Krevor, S.C.M., Ide, T., Benson, S.M., Franklin M. Orr, J., 2011. Real-time tracking of CO_2 injected into a subsurface coal fire through high-frequency measurements of the $^{13}CO_2$ signature. Environ. Sci. Technol. 45, 4176-4186.

Kuenzer, C., Stracher, G.B., 2012. Geomorphology of coal seam fires. Geomorphology 138, 209-222.

Kuenzer, C., Zhang, J., Tetzlaff, A., van Dijk, P., Voigt, S., Mehl, H., Wagner, W., 2007. Uncontrolled coal fires and their enviornmental impacts: Investigating two arid mining regions in north-central China. Appl. Geogr. 27, 42-62.

Li, J., Fu, P., Zhu, Q., Mao, Y., Yang, C., 2018. A lab-scale experiment on low-temperature coal oxidation in context of underground coal fires. Appl. Therm. Eng. 141, 333-338.

O'Keefe, J.M., Henke, K.R., Hower, J.C., Engle, M.A., Stracher, G.B., Stucker, J., Drew, J.W., Staggs, W.D., Murray, T.M., Hammond III, M.L., 2010. CO_2, CO, and Hg emissions from the Truman Shepherd and Ruth Mullins coal fires, eastern Kentucky, USA. Sci. Total Environ. 408, 1628-1633.

O'Keefe, J.M.K., Neace, E.R., Lemley, E.W., Hower, J.C., Henke, K.R., Copley, G., Hatch, R.S., Satterwhite, A.B., Blake, D.R., 2011. Old Smokey coal fire, Floyd County, Kentucky: Estimates of gaseous emission rates. Int. J. Coal Geol. 87, 150-156.

Rein, G., 2011. Smoldering combustion phenomena and coal fires. In: Stracher, G.B., Prakash, A., Sokol, E.V. (Eds.), Coal and Peat Fires: A Global Perspective: Coal-Geology and Combustion. Elsevier, pp. 307-315.

Rein, G., 2013. Smouldering fires and natural fuels. In: Belcher, C. (Ed.), Fire Phenomena and the Earth System: An Interdisciplinary Guide to Fire Science. Wiley and Sons, pp. 15-34.

Rein, G., 2016. Smoldering combustion. In: SFPE Handbook of Fire Protection Engineering. Springer, pp. 581-603.

Schloemer, S., 2006. Gas and temperature measurements at fire zones 3.2 & 8. Unpublished Project Report as a Contribution to the Sino-German Research Initiative 'Innovative Technologies for Exploration, Extinction and Monitoring of Coal Fire in North China'. Federal Institute for Geosciences and Natural Resources (BGR), Hannover, Germany.

Shi, B., Su, H., Li, J., Qi, H., Zhou, F., Torero, J.L., Chen, Z., 2017. Clean power generation from the intractable natural coalfield fires: Turn harm into benefit. Sci. Rep. 7, 5302.

Song, Z., Fan, H., Jiang, J., Li, C., 2017a. Insight into effects of pore diffusion on smoldering kinetics of coal using a 4-step chemical reaction model. J. Loss Prevent. Proc. 48, 312-319.

Song, Z., Huang, X., Luo, M., Gong, J., Pan, X., 2017b. Experimental study on the diffusion-kinetics interaction in heterogeneous reaction of coal. J. Therm. Anal. Calorim. 127, 1625-1637.

Song, Z., Kuenzer, C., 2014. Coal fires in China over the last decade: A comprehensive review. Int. J. Coal Geol. 133, 72-99.

Song, Z., Huang, X., Kuenzer, C., Zhu, H., Jiang, J., Pan, X., Zhong, X., 2019a. Chimney effect induced by smoldering fire in a U-shaped porous channel: A governing mechanism of the persistent underground coal fires. Process. Saf. Environ. Prot., Revision.

Song, Z., Wu, D., Jiang, J., Pan, X., 2019b. Thermo-solutal buoyancy driven air flow through thermally decomposed thin porous media in a U-shaped channel: Towards understanding persistent underground coal fires. Appl. Therm. Eng. 159, 113948.

Song, Z., Zhu, H., Tan, B., Wang, H., Qin, X., 2014. Numerical study on effects of air leakages from abandoned galleries on hill-side coal fires. Fire Saf. J. 69, 99-110.

Song, Z., Zhu, H., Xu, J., Qin, X., 2015. Effects of atmospheric pressure fluctuations on hill-side coal fires and surface anomalies. Int. J. Min. Sci. Technol. 25, 1037-1044.

Switzer, C., ., Pironi, P., ., Gerhard, J.I., Rein, G., ., Torero, J.L., 2009. Self-sustaining smoldering combustion: a novel remediation process for non-aqueous-phase liquids in porous media. Environ. Sci. Technol. 43, 5871-5877.

Switzer, C., Pironi, P., Gerhard, J.I., Rein, G., Torero, J.L., 2014. Volumetric scale-up of smouldering remediation of contaminated materials. J. Hazard. Mater. 268, 51-60.

Tetzlaff, A., 2004. Coal Fire Quantification Using Aster, ETM and Bird Satellite Instrument Data. Ludwig-Maximilians-University, Munich.

Torero, J.L., Fernandez-Pello, A.C., 1996. Forward smolder of polyurethane foam in a forced air flow. Combust. Flame 106, 89-109.

van Dijk, P., Zhang, J., Jun, W., Kuenzer, C., Wolf, K.-H., 2011. Assessment of the contribution of in-situ combustion of coal to greenhouse gas emission; based on a comparison of Chinese mining information to previous remote sensing estimates. Int. J. Coal Geol. 86, 108-119.

Wu, D., Schmidt, M., Huang, X., Verplaetsen, F., 2017. Self-ignition and smoldering characteristics of coal dust accumulations in O_2/N_2 and O_2/CO_2 atmospheres. Proc. Combust. Inst. 36, 3195-3202.

Yang, J., Chen, H., Liu, N., 2016. Modeling of Two-Dimensional Natural Downward Smoldering of Peat. Energy Fuels 30, 8765-8775.

Yang, J., Liu, N., Chen, H., Gao, W., Tu, R., 2019. Effects of atmospheric oxygen on horizontal peat smoldering fires: Experimental and numerical study. Proc. Combust. Inst. 37, 4063-4071.

Yuan, L., Smith, A.C., 2011. CO and CO_2 emissions from spontaneous heating of coal under different ventilation rates. Int. J. Coal Geol. 88, 24-30.

Zanoni, M.A.B., Torero, J.L., Gerhard, J.I., 2019a. Delineating and explaining the limits of self-sustained smouldering combustion. Combust. Flame 201, 78-92.

Zanoni, M.A.B., Torero, J.L., Gerhard, J.I., 2019b. Determining the conditions that lead to self-sustained smouldering combustion by means of numerical modelling. Proc. Combust. Inst. 37, 4043-4051.

Zanoni, M.A.B., Torero, J.L., Gerhard, J.I., 2019c. The role of local thermal non-equilibrium in modelling smouldering combustion of organic liquids. Proc. Combust. Inst. 37, 3109-3117.